International Research Journal of Engineering and Technology (IRJET) e-ISSN: 2395-0056
Volume: 08 Issue: 09 | Sep 2021 www.irjet.net p-ISSN: 2395-0072

Performance of Al-Al_2O_3 Composites under Coupled Mechanical and Thermal Stimuli

Pradeep Gudlur[1,*], Miladin Radovic[2,3] and Anastasia Muliana[2]

[1]*Department of Mechanical Engineering, Union College, USA*
[2]*Department of Mechanical Engineering, Texas A&M University, USA*
[3]*Department of Materials Science and Engineering, Texas A&M University, USA*

Abstract - This study aims at understanding the performance of Al-Al_2O_3 composites subjected to uniaxial compressive loading at several isothermal temperatures (25, 200 and 400 ^oC). Two types of composites are considered. The first composite system consists of uniform distributions of the Al and Al_2O_3 constituents, with 0, 5 and 10 vol% of Al_2O_3 randomly distributed in Al matrix. The second system includes gradual variations in the compositions of the Al and Al_2O_3 constituents, i.e., layers of composites with 0, 5 and 10 vol% of Al_2O_3 are stacked together to form a functionally graded composite (FGC). Compression tests were conducted to 5% strain under the constant displacement rate, followed by removal of the loads, which result in permanent (plastic) deformation of composites. The corresponding stress-strain responses were used to examine the effects of temperature, volume fraction of Al_2O_3, porosity, distribution and composition of the constituents on the overall performance and mechanical properties of these composites. As expected, the magnitudes of the elastic moduli and yield stresses decreased with increase in temperatures and porosity. The elastic moduli determined from the compression testing of the composites with uniform distributions of constituents are compared with those obtained from Resonant Ultrasound Spectroscopy to examine the elastic response of the composite. The FGC samples showed an almost identical response with those of 0% samples in the elastic region. However, the FGCs showed slightly more net strain hardening than the 0% samples. Drop in modulus with temperature rise was higher for the normal composite samples than the FGCs.

Keywords: Aluminum composites; functionally graded; mechanical testing; powder processing; strain hardening parameters

1. Introduction

Ceramic particles are often used to reinforce metals to form ceramic particulate metal matrix composites (CPMMCs). CPMMCs have relatively high strength and stiffness, since the stiffer ceramics can improve the overall stiffness, and the combinations of brittle and ductile constituents can enhance the compressive strength and failure strain of the composites. Good bonding at the interface of ceramic particles and metal matrix needs to be maintained in order to significantly improve the performance of the CPMMC. Aluminum reinforced with alumina is a good choice for CPMMC, because of their good wettability [1] and lack of interfacial reaction between them (alumina is stable inside the aluminum matrix [2]). Al-Al_2O_3 composites are widely used in many engineering applications because of their appealing properties, i.e., high modulus to density ratio, high stiffness, low wear rate and high coefficient of friction. Hence they find applications in (a) automotive components e.g. brake discs, drums, back-plate, engine block, piston and gearbox parts [3, 4], (b) aerospace vehicles e.g. fans in gas turbine engine, rotating blade sleeves in helicopters and flight control hydraulic manifolds [3], (c) kitchen utilities e.g. food and beverages packing and (d) sports applications e.g. bikes and golf components [3].

Though ceramics and metals have significant differences in their thermo-mechanical and physical properties, it is well documented in literature that aluminum and alumina adhere strongly to each other without the presence of any thin intermediate transition layers. Saiz et al. [1] studied the wetting properties, strength and the interface characteristics of Al-Al_2O_3. They found that Al and Al_2O_3 form a very strong interface when joined in solid state, i.e., when Al was not a molten liquid during processing, and the interface bonding strength increased with increase in the bonding temperature. Highest strength was obtained when the bonding temperature was close to the melting temperature of aluminum (650 ^oC); and beyond the melting point, bonding strength was observed to decrease. Saiz et al. [1] and Timsit et al. [5] noticed the presence of unbonded regions at the interface, which were identified by EDS (Energy Dispersive Xray Spectroscopy) and HREM (High Resolution Electron Microscopy) as amorphous aluminum oxide, formed as islands close to the interface due to oxidation of aluminum. These aluminum oxide islands decreased the strength of the interface; however, the number of aluminum oxide islands

were observed to decrease when the bonding temperature was brought close to the melting temperature of aluminum. These aluminum oxide islands were twice as tall as the interplanar spacing of aluminum, making the interface extremely rough with short irregular ledges.

Common processing methods to manufacture Al-Al_2O_3 composites are squeeze casting (also called as metal infiltration), reactive processing, spray deposition and powder metallurgy. Of all these methods, powder metallurgy is the most commonly used method because it is easier to control the distribution of alumina particles in aluminum matrix and obtain practically any shape of the composite samples, by merely using different shapes of the die. Finally, this method is relatively inexpensive. The disadvantage of using powder metallurgy method compared to other methods is that there is imminent problem with porosity as a result of incomplete sintering, which is also observed in this study.

Substantial number of experimental studies have been conducted on understanding the mechanical performance of Al-Al_2O_3 composites, with a relatively uniform distribution of alumina particles in the aluminum matrix. Ali Hubi et al. [6] manufactured Al-Al_2O_3 composites using powder metallurgy method with varying Al_2O_3 (3, 6, 9 and 12 wt%) and determined the compressive strength and Brinell hardness at room temperature. They found that for the 12 wt% Al_2O_3 reinforced composite, there was an increase of 54% in the compressive strength and 89% increase in the Brinell hardness from those of the unreinforced aluminum samples. Kouzeli and Dunand [7] manufactured Al-Al_2O_3 composite samples with varying Al_2O_3 (34 to 37 vol %) using metal infiltration method. They conducted uniaxial compression tests at different temperatures (25 ^oC to 600 ^oC) and at several strain rates (10^{-3} to 1 s^{-1}). They found that the composite samples exhibited a significant increase in strength when compared to the pure aluminum sample, mainly because of an increase in flow stresses, which were attributed to two mechanisms, viz., direct strengthening (because of load sharing between the ceramic particles and metal matrix) and forest hardening (because of interactions between forest dislocations). Ganguly [8] conducted uniaxial tensile and compression testing on Al-Al_2O_3 composites at three different temperatures 300 ^oC, 425 ^oC and 550 ^oC, and showed that the dominant failure mechanism was particle cracking at low temperature (300 ^oC), whereas at high temperature (550 ^oC) the dominant failure mechanism was interfacial decohesion. In between 300 ^oC and 550 ^oC both particle cracking and interfacial decohesion were observed. The effect of strain rate on the overall ductility or failure strain of the composites was negligible, however higher strain rates lead to failure due to particle cracking. The composite sample was less prone to particle cracking at higher temperatures or lower strain rates because an increase in temperature or a decrease in strain rate leads to lower flow stresses in the aluminum, in turn resulting in lower stresses in alumina particles. Ductility was reduced when there were particle clusters in the composite sample, as damage occurred through coalescence of voids near the particle clusters. Gudlur et al. [9] studied the overall elastic and mechanical response of Al-Al_2O_3 composites using Resonant Ultrasound Spectroscopy (RUS) and uniaxial compression testing. The overall response of aluminium-alumina (Al-Al_2O_3) composites was found to depend strongly on their microstructural characteristics. The effects of processing, porosity, alumina content, thermal (residual) stress, and plastic deformation on the overall elastic modulus and response of the composites were also studied. By altering the processing method slightly, they observed a significant effect of processing conditions on the microstructural characteristics and in turn on the overall physical and mechanical properties of the composite. Furthermore, with changes in porosity by 2-3%, the elastic moduli were found to vary by 10-15 GPa.

Another type of composite systems is a functionally graded composite (FGC). FGCs are useful when, for example, one end of the material needs to withstand harsh environments and the other end of the material needs to be connected to a substrate/base material (e.g. metal) that is to be protected from those harsh environments. The most common FGCs are in the form of ceramic particle reinforced metal matrix composites in which the ceramic composition is spatially varied in a controlled manner to obtain the desired spatial variation of macroscopic properties. Various methods have been considered for manufacturing FGCs. Die Compacting (also called as Powder Stacking) is one of the earliest and simplest methods in which powders having different compositions are stacked one over the other as layers, cold compacted and later sintered [10]. The disadvantages of this method are: (a) the gradient distribution may not be smooth (as compaction and sintering stages can alter the distribution) and (b) the size of the FGC and the number of layers are limited by the size of the die used [11]. However, this method involves fewer costs and can be used in laboratory to study the overall thermo-mechanical properties of the FGC. For commercial purposes more advanced processing methods are used for fabricating FGCs, such as centrifugal stir casting [12], centrifugal sedimentation [13, 14], physical vapor deposition [15] and chemical vapor deposition [16].

Shabana et al. [17] used die compaction method followed by pressure-less sintering method to manufacture Ni-Al_2O_3 FGC. They studied the shrinkage differences between different layers during the sintering process, which alter the distribution and development of stresses, crack

initiation and delamination in the FGCs. Rajan et al. [12] manufactured Al-SiC FGCs as thick hollow cylinders using centrifugal stir casting method and measured the hardness variation in the radial direction from 115 BHN to 145 BHN when the SiC composition varied gradually from 0 to 40vol%. Fukui et al. [18] manufactured Al-Al_3Ni FGC samples by centrifugal casting method. Using a combination of rule of mixtures and flexural forced resonant frequency method, they measured the elastic moduli of the FGC samples to vary from 81 and 101 GPa in the gradient direction corresponding to 15.2 and 43.2 vol% of Al_3Ni. Ben-Oumrane et al. [19] used theoretical methods to determine the displacement and axial stress distribution in bending of Al-Al_2O_3 FGC thick beams. As expected, they observed larger deflections in the Al rich areas than in the ceramic rich area of the beams. They also found that the axial stress distribution varies with the beam thickness, i.e., a linear variation was seen in pure Al beam and a nonlinear variation was observed for the FGC.

The main focus of this study is to examine the effects of temperature, volume fraction of Al_2O_3, variation in the constituent compositions, and porosity on the overall mechanical performance and properties of Al-Al_2O_3 composites. Two composite systems with uniform distribution and non-uniform distribution of Al_2O_3 particles in an aluminum matrix; the later one commonly known as functionally graded composites are considered. Both systems are manufactured using powder metallurgy method. We then conduct uniaxial compressive testing by loading the samples up to 5% strain at different temperatures: 25, 200, and 400 ^oC and determine the mechanical properties and overall behaviors of the composites from the stress-strain responses.

2. Experimental Methodology

a) Fabrication of Al-Al_2O_3 composite samples: Al-Al_2O_3 samples were prepared using powder metallurgy method, as described in Gudlur et al. in more detail [20]. The composites were made with 99.5% pure aluminum powder of -100+325 mesh size (Alfa Aesar, MA) and 99.7% pure alumina (Sigma-Aldrich, MO). The aluminum particles appeared to be mostly spherical and varied in size approximately between 1 m and 50 m in diameter whereas the alumina particles were about 10 m and were polygonal in shape. A 12.7 mm dry pressing die was used to prepare the samples and care has been taken to limit porosity to as little as possible as described in Gudlur et al. [20]. Proper amounts of Al and Al_2O_3 powders were mixed using a ball milling, and cold pressed in cylindrical die using a hydraulic press at uniaxial pressure of 502 MPa for 30 minutes at room temperature. The cold pressed pallets were further sintered in a quartz furnace (GSL-1100X, MTI, CA) at 600 ^oC. The samples were heated from room temperature to 600 ^oC at a rate of 5 ^oC/min, and sintered at that temperature for 2 hours, and then cooled back naturally to room temperature. The top and bottom surfaces of the sample need to be flat and parallel in order to obtain the uniaxial stress-strain curves and eliminate the effect of bending and stress concentration due to uneven surfaces. Firstly, the ends of the sample were machined in lathe followed by polishing using finer sand paper to get flat and parallel contact surfaces. To minimize the friction and barreling effects, Silicone based lubricant was used between the surfaces of compression platens and samples. The composite samples with 0, 5 and 10 vol% alumina concentrations were subjected to compression testing at room temperature (25 ^oC) and elevated temperatures (200 ^oC and 400 ^oC). Composite specimens which were cylindrical in shape with dimensions of (12.7 mm in diameter) × (23.87±1.778 mm in height), with height to diameter ratio varying from 1.72 to 2.0, were used for compression testing. X-ray Diffraction, XRD, (Bruker-AXS D8 Advanced Bragg-Brentano X-ray Powder Diffractometer, Bruker, WI) was used to identify the constituents present in the composite and the vol% of each constituent in the composite. The sample surface was scanned from $2\theta=20^0$ to $2\theta=70^0$ with a step size of 0.015^0 at a rate of 0.0375 degrees/sec; and LynxEye detector was used to record the XRD patterns. As the volume content of alumina increases the height (intensity) of aluminum peaks decreases whereas height of alumina peaks increases. Detailed discussion on analyzing the constituent compositions and volume content of the alumina in the composites using XRD is given in Gudlur et al. [9, 20]. Table 1 shows the dimensions of the composite samples used in this study. Porosity present in each sample was determined using Archimedes' principle and the reported percent porosity combines both open and closed porosities. Detailed discussion on the amount of open and closed porosities in the samples can be found in Gudlur et al. [9, 20].

b) Fabrication of functionally graded Al-Al_2O_3 composite samples: Al- Al_2O_3 FGC samples were manufactured using die compacting (also called as Powder stacking) method by stacking different powders with different compositions of Al and Al_2O_3 one over the other as layers and compacting them all at once. FGC samples were prepared by adding 2.8 grams of 0, 5 and 10 vol% composite powders each to a 12.7 mm die one layer above another just by tapping them. Once all the layers of powder were added to the die, a compacting pressure of 502 MPa was applied. The compacted cylindrical FGC pallet was then sintered at 600 ^oC for 2 hours in an argon environment, following the procedures used to manufacture composite samples discussed in Gudlur et al. [20].

c) Compression testing setup: The MTS 810 servo-hydraulic testing system and a high temperature extensometer with gauge length of 15.24 mm (both from MTS Systems Corporation, MN), were used for compression testing in this study. Displacement control mode was used to compress the prepared Al-Al_2O_3 composite samples in the MTS machine at

the constant displacement rate of 1.25 mm/min. Axial displacements along with axial loads were recorded during the loading stage using extensometer and load cell. The axial normal strain was determined by normalizing the applied displacement with respect to the overall height of the sample, and the normal stress was calculated as the recorded force divided by the original area of the cross-section. Once 5% strain was reached, the samples were unloaded at the same displacement rate (crossheads were moved away from each other) until the recorded force reached zero. The axial stress and axial strain during the unloading step were again recorded using the load cell and extensometer data, respectively. The uniaxial compressive stress-strain curves were thus plotted in terms of engineering stresses and strains.

3. Uniaxial compressive stress-strain behavior of Al-Al_2O_3 composites

Figures 1a-c show the stress strain curves of Al-Al_2O_3 composites under uniaxial compressive testing at three different temperatures 25, 200 and 400 ^oC. At each testing temperature, two composite samples of each composition, i.e. 0, 5 and 10% volume fraction of alumina, were tested. The physical attributes of the composite samples (viz. volume fraction of alumina determined from XRD, % porosity) are listed in Table 1. It can be seen from Figures 1a-c that as the testing temperature increased, the stress strain curves dropped significantly for all composite samples with different volume fractions. This behavior is expected because with an increase in temperature the material becomes softer and the dislocation motion becomes easier and hence, the flow resistance of the material decreases at higher temperatures. On the other hand, there was only slight variation in the stress strain curves with increase in volume fraction of the tested composites. As amounts of alumina particles increase, higher porosity was seen in the composites (see Table 1), which increase the internal stresses in the constituents, thus only slightly higher loads (overall stresses) were recorded in the composites with higher alumina contents for the same level of strains. In other words, expected strengthening by addition of larger fraction of Al_2O_3 was diminished by introduction of larger volume fraction of porosity.

The stress strain curves at different temperatures, volume fraction of alumina and microstructure was approximated by using an empirical model and discussed further by characterizing the elastic modulus, yield stress, strain hardening coefficient (n) and strengthening coefficient (K) of the composite samples. The elastic modulus and yield stress of the composite samples tested at various temperatures were determined from the stress strain curves. During the loading step, it was observed that all curves showed nonlinear elastic behavior with only a small portion of the curves appearing to be linear, most likely because of the uneven surfaces or slight misalignment of the sample and fixture initially during loading. Therefore, the elastic modulus E* reported in Table 1 was determined during the unloading step by taking the slope of stress and strain curve [21]. Unloading was done until the recorded force in the composite material was zero (until the cross heads lost contact with the sample), but there was still some residual strain present in the composite because of undergoing plastic deformations during the loading stage, and hence the stress-strain curves did not go back to the original state completely. The unloading portion of the stress-strain curve shows the residual strain and elastic strain recovery of the composite samples. For determining the yield stress, first a line was drawn at 0.2% stain with the elastic modulus of the composite sample as its slope, and then the stress corresponding to the intersection of this line with the stress-strain curve was noted down as the yield stress of the composite sample. Table 1 summarizes the corresponding elastic modulus and yield stress of the composite samples obtained from their stress-strain curves.

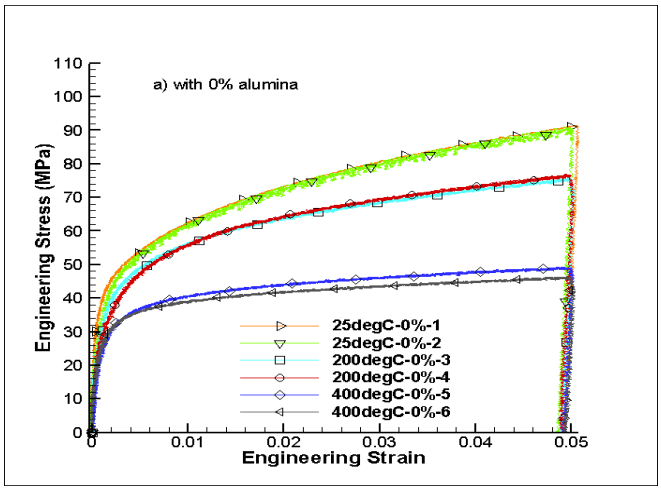

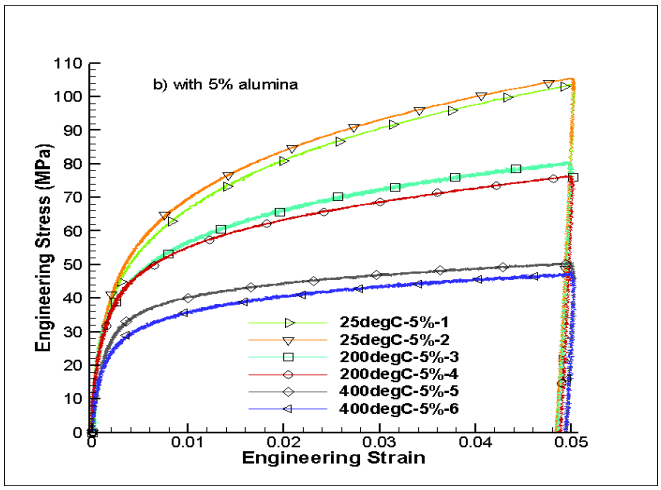

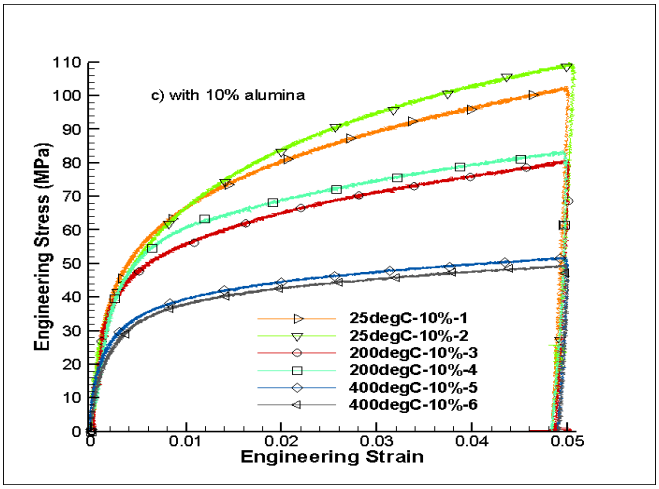

Figure 1. Stress-strain response of composite samples with a) 0% b) 5% and c) 10% alumina volume contents at various temperatures

Table 1. Composite samples tested at various temperatures and their physical and mechanical properties.

Test temp ^{0}C	Sample	V.F	Porosity %	E* GPa	σ_{yield} MPa	$\sigma_T = K\,\varepsilon_T^n$	
						K MPa	n
25	0%-1	0.9	4.22	61.2	50	193.6	0.24
	0%-2	1.1	4.29	56.0	46	199.1	0.25
	5%-1	6.7	5.90	55.5	44	272.4	0.30
	5%-2	6.4	5.32	56.9	46	268.3	0.29
	10%-1	11.9	9.63	57.9	42	254.0	0.30
	10%-2	11.6	6.15	55.5	38	328.2	0.36
200	0%-3	1.6	4.65	55.9	43	146.0	0.21
	0%-4	1.4	3.6	51.1	39	160.0	0.23
	5%-3	5.9	4.73	51.0	41	177.6	0.25
	5%-4	6.3	6.10	55.4	39	158.4	0.23
	10%-3	11.2	6.62	53.3	43	164.2	0.23
	10%-4	11.4	5.71	51.2	40	177.6	0.24
400	0%-5	1.5	3.75	42.8	32	79.2	0.14
	0%-6	1.7	4.65	43.7	33	69.9	0.13
	5%-5	6.9	4.82	45.6	30	88.7	0.17
	5%-6	7.0	4.90	42.8	26	91.8	0.20
	10%-5	11.7	7.03	44.6	28	99.9	0.20
	10%-6	12.2	7.63	44.8	25	974	0.20

From Table 1, the average elastic modulus and yield stress for each volume fraction of composite sample were calculated along with their standard deviation. Figures 2a-b show the variation of the average elastic modulus and average yield stress with temperature, porosity and volume fraction of alumina in examined composites. The modulus and yield stress of the composite samples decreased drastically with increase in temperature because of softening, increase in atomic vibrations and dislocation movement at higher temperatures. Further, it was also seen from Table 1 that both modulus and yield stress decreased with increase in volume fraction of alumina, which was against our expectations, as alumina has higher elastic modulus than aluminum. The reason for this trend can be attributed to the fact that an increase in volume fraction of alumina resulted in an increase in porosity, as summarized in Table 1. For the same height and diameter of the composite specimens, as the volume fraction of alumina in the composite samples increased, it became more difficult to manufacture them without introducing substantial porosity than those of the unreinforced 0% composite sample [20]. Therefore, different processing methods might be necessary to manufacture Al-Al_2O_3 composites with high volume contents of alumina and low porosity contents, if the goal is to increase the modulus with the addition of ceramic particles.

The yield stress (σ_{yield}) indicates the onset of plastic deformations. The composite material undergoes strain hardening (stress required to maintain the flow increases with increasing strain) after the yield point, and the stress at which continuous plastic deformation occurs is called as flow stress. Equation 1 shows the empirical model of the flow stress as a function of strain. To define the behavior of composites in the strain-hardening region, it is necessary to find the strain hardening coefficient (n) and strengthening coefficient (K) in the empirical Equation 1. The true stress (σ_T) and strain (ϵ_T) values are used for this purpose and are calculated from the yield point to the 5% strain using Equation 2.

$$\text{Flow curve: } \sigma_T = K\,\varepsilon_T^n \qquad (1)$$

$$\log \sigma_T = \log K + n \log \varepsilon_T$$
$$\sigma_T = \sigma_e(1 + \varepsilon_e) \text{ and } \varepsilon_T = \ln(1 + \varepsilon_e) \quad (2)$$

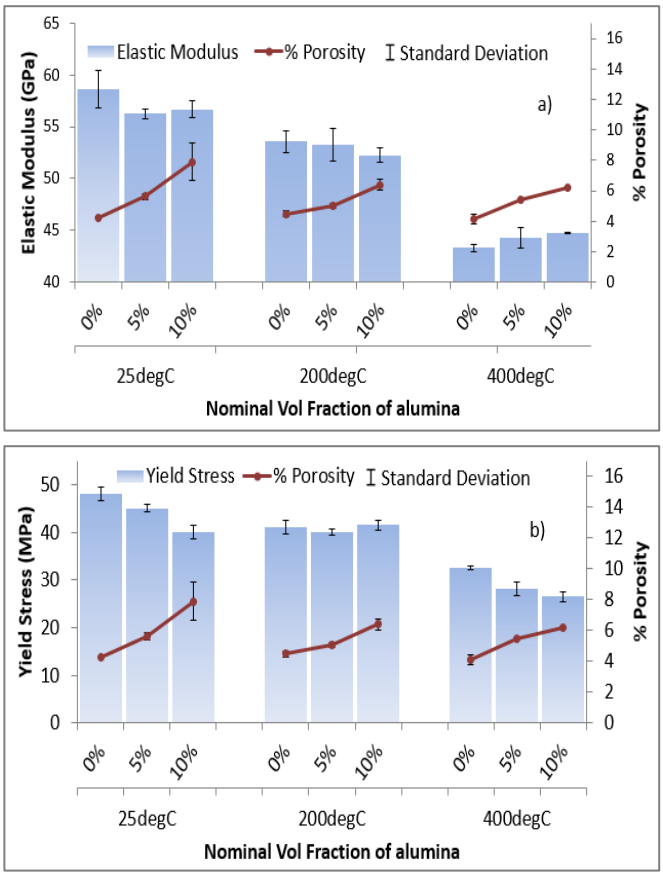

Figure 2. Effect of temperature, porosity and volume fraction on a) elastic modulus and b) yield stress of composite samples

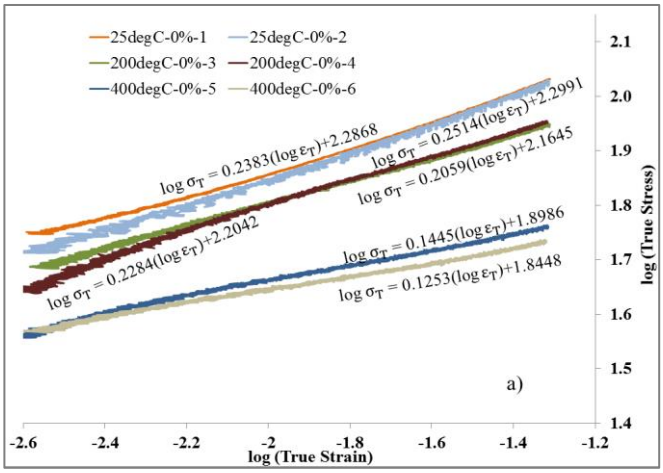

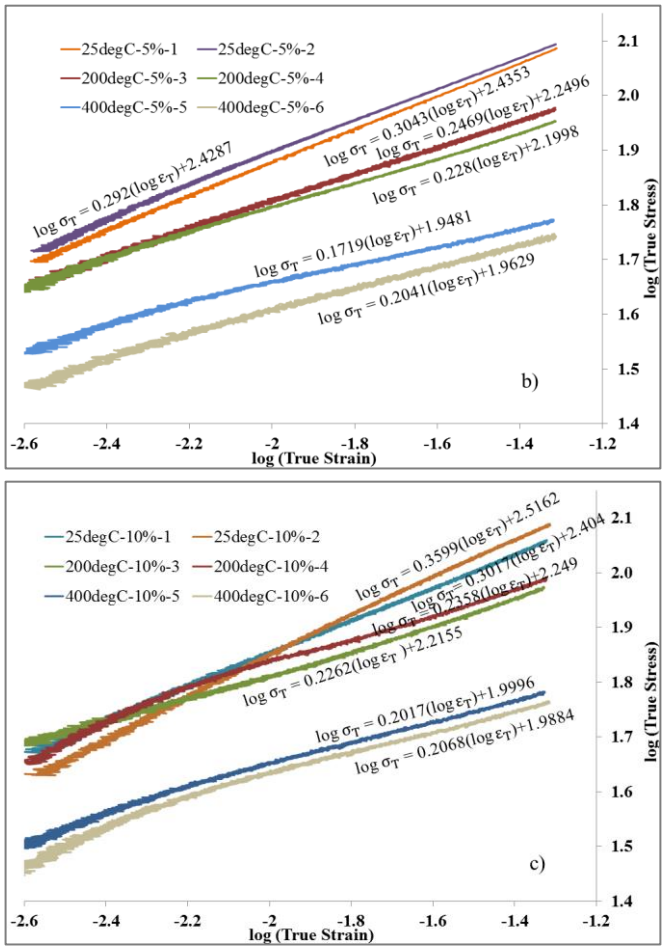

Figure 3. Determination of n and K from the true stress strain curves for a) 0% b) 5% and c) 10% composite samples at various temperatures

Figures 3a-c depict the procedure used to determine the strain hardening coefficient (n) and strengthening coefficient (K) from the log(true stress) vs. log(true strain) curves of 0, 5 and 10 vol% composite samples at various temperatures, respectively. The strain hardening coefficient (n) is the slope of the log(true stress) vs. log(true strain); whereas the strengthening coefficient (K) is the true stress for true strain=1, or in other words log(K) is the y-intercept of the log(true stress) vs. log(true strain) curve. Table 1 summaries n and K values for different composite samples.

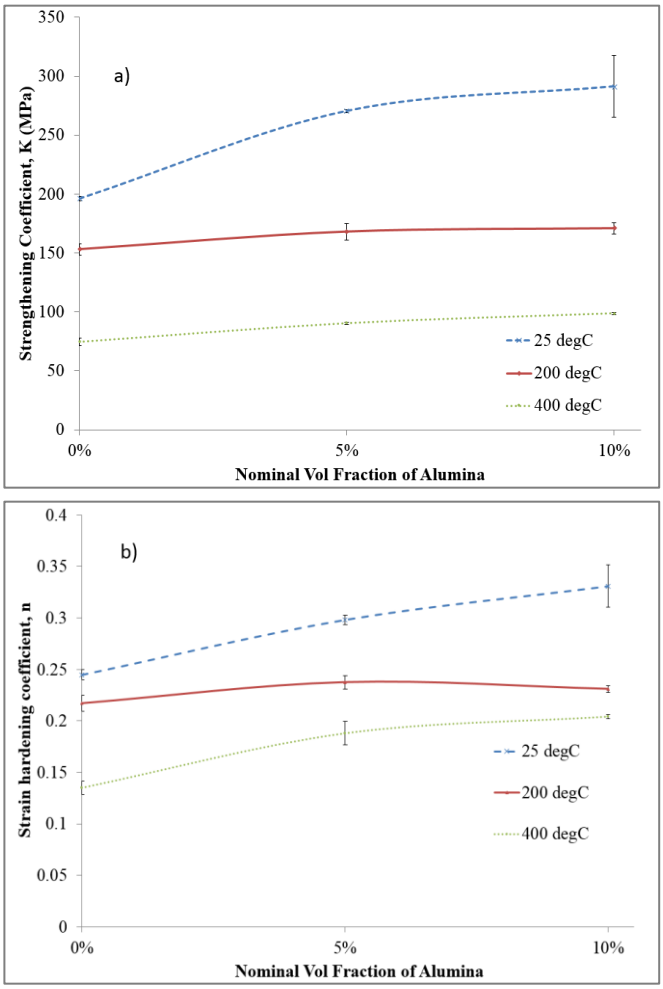

Figure 4. Variation of a) Strengthening coefficient (K) and b) Strain hardening coefficient (n) with compression testing temperature and volume fraction of the composite

Figure 4 shows the variation of strengthening coefficient (K) and strain hardening coefficient (n) with compression testing temperature and volume fraction of the composite. Both n and K decreased with increase in temperature as expected. This is due to an increase in the dislocation mobility at higher temperatures making it easier for the materials to undergo plastic deformations with relatively small strain hardening. With an increase in volume fraction, the n and K values increased slightly due to the hindrance for dislocation motion provided by the alumina reinforcement. The strain hardening coefficient lies between 0 (for perfectly plastic material) and 1 (for perfectly elastic material), as discussed in [22]. Low n and K values means the material has less tendency to strain harden and requires lower stresses to undergo plastic deformation; and high n and K values means pronounced strain hardening behaviors in the material [23]. Totten and MacKenzie [24] reported that for commercial aluminum alloys, n and K were usually found to lie between 0.18-0.24 and 146-479 MPa, respectively, at room temperature. For the studied Al-Al_2O_3 composites, we found n and K to vary between 0.23-0.35 and 193-328 MPa, respectively, (see Table 1) at room temperature.

Table 2. Composite samples with 10% nominal Al2O3 volume content used for RUS, their porosity, alumina content, and elastic modulus

Sample	Porosity (%)	Alumina content (%)	Modulus (GPa)
RUS-10-1	6.03	13.4	62.41
RUS-10-2	7.37	13.5	61.60
RUS-10-3	6.89	12.2	58.58
Average			60.86 ± 2.02

Table 3. Measured alumina content and porosity of composite samples with 10% nominal Al_2O_3 volume content used for compression testing

Sample	Porosity (%)	Alumina content (%)	Modulus (GPa)
CT-10-1	6.31	11.5	60.90
CT-10-2	6.49	11.2	51.40
CT-10-3	7.34	11.7	55.40
CT-10-4	6.07	11.4	62.24
Average			57.49±5.02

Next, the elastic moduli obtained from the compression testing (CT) are compared to the ones determined from Resonant Ultrasound spectroscopy (RUS) in Table 2. RUS is a dynamic nondestructive testing method used to determine the elastic properties of solid objects (metals, ceramics or composites), by measuring the natural frequencies of the samples. Radovic et al. [25] has shown that RUS is more accurate in determining the elastic properties than conventional static testing methods because RUS requires low amplitude loading, which makes it possible for a reliable determination of the linear elastic moduli. Unlike the conventional testing methods, RUS is a great tool to determine all the components of stiffness tensor in one run, even if the material is anisotropic. In this study, the purpose of conducting RUS is to validate the elastic moduli determined from the unloading part of the stress-strain curves under compressive stresses. This will also confirm

that the elastic recovery response during removal of the loads. For the RUS samples, powder metallurgy method was also used; however, the dimensions of the specimens are 5mm in diameter and 7mm in thickness. The composite pallets were placed on 3 transducers of which one of them was sending out an ultrasonic wave and the other two transducers recorded the natural frequencies at which the sample was vibrating. For determining the elastic moduli of the composite material from resonant spectra, a set of "guessed" elastic constants were given to calculate an approximate spectrum. Multidimensional software Quasar RuSpec (Magnaflux Quasar Systems, Albuquerque, NM) iteratively minimizes error between the measured and calculated resonant peaks by changing the trial elastic constants. Detailed discussion on conducting RUS test can be found in Gudlur et al. [21]. Table 2 shows the physical properties of the composite samples with 10% Al_2O_3 volume content used for RUS along with their elastic moduli obtained from RUS at room temperature. To further illustrate the results, %porosity and elastic moduli for the 10 vol% composite from the uniaxial compression tests (CT) are summarized in Table 3. All properties were measured at room temperature. From Tables 2 and 3, it is seen that the elastic moduli determined from the unloading part of the compressive tests are comparable to the ones obtained from RUS. This confirms the elastic recovery response during unloading. Slightly lower modulus measured in CT can be attributed to the slightly lower alumina content in those samples when compared to RUS samples.

4. Uniaxial compressive stress-strain behavior of Al-Al_2O_3 functionally graded composites (FGC)

Figure 5 shows the SEM images of an FGC sample taken at various locations along the graded direction (longitudinal axis). Al_2O_3 composition varies gradually along the longitudinal axis from right to left. Figure 6 shows selected, but typical stress strain curves of Al-Al_2O_3 FGC samples at three different isothermal temperatures 25, 200 and 400 ^oC. It is noted that the reported stress is obtained by dividing the applied uniaxial force by the original area. In the FGC samples, the reported normal strain is defined as the net uniaxial contraction divided by the initial length of the FGC samples, which is not necessarily the same as the axial strains present in each layer in the FGC samples. The force was applied along the grading direction. For the uniaxial case, the normal stresses at each location along the grading direction are equal to this reported axial stress. At each testing temperature, two FGC samples were tested at a displacement rate of 1.25 mm/min, which is the same rate as testing the Al_2O_3 composite samples, until it reaches 5% strain followed by removal of the stresses. In the FGC sample, material properties change with the locations, leading to different deformations under the same stresses. The physical attributes of the FGC samples tested (viz. mass, dimensions and overall % porosity) are listed in Table 4. The stress-strain curves of aluminum matrix under compressive stresses at various temperatures are also added in Figure 6 for comparison. It can be seen from Figure 6 that as the testing temperature increased, the stress strain curves dropped significantly both for FGC and composite samples, which is expected. The FGC samples have almost identical response in the elastic region when compared to those of 0% composite samples. However, the FGC samples experience slightly higher strain hardening effect than the 0% samples, because of the hindrance provided by the alumina reinforcement to plastic deformation in the FGC samples. For conducting compression tests, we needed samples longer than 22.86 mm (0.9 inches), so that extensometer with gauge length of 15.24 mm (0.6 inches) could be connected. During cold pressing of powders, it was difficult to make thin and long samples (with length greater than 22.86 mm, using a die of 12.7 mm diameter) as volume fraction in the composite increases. Cold pressing of higher volume fraction (15, 20 or 25 vol%) composites resulted in samples having their edges torn off and any polishing the samples to get flat surfaces resulted in shorter samples making them not suitable for compression testing. We faced a similar problem when manufacturing FGC samples with higher volume fraction alumina layers. Hence for compression testing, because of the specimen's length/diameter requirements, only 0, 5 and 10 vol% composites were manufactured and used for compression testing.

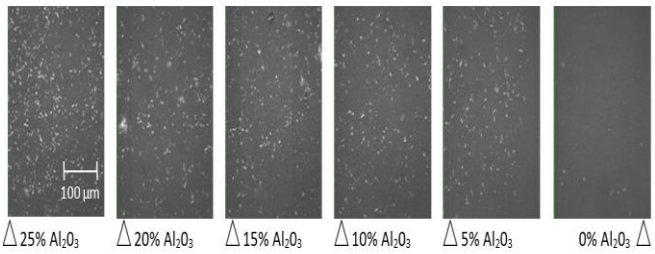

Figure 5. SEM image of FGC sample at various locations along the cylindrical axis

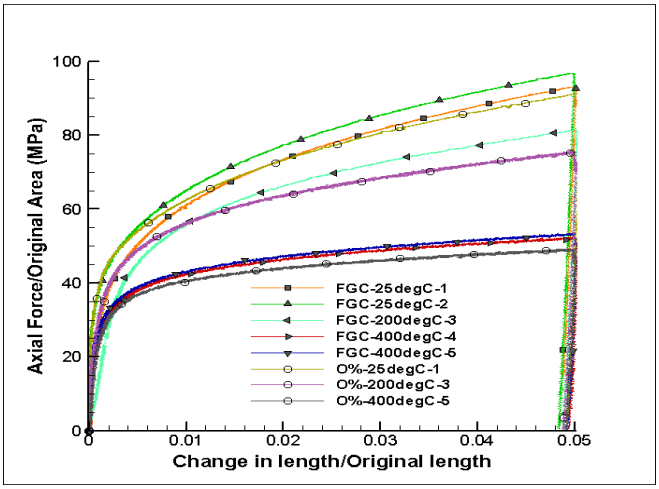

Figure 6. Stress Strain behavior of FGC samples along with 0% composite samples

The overall (net) elastic modulus and yield stress of the FGC samples tested at various temperatures are determined from the stress strain curves. It should be noted that in the FGC samples, we determine the overall modulus as the ratio of the normalized force (force/original area) to the normalized displacement (change in length over the original length), which is not the same as the modulus that relates the local stress to the local strain in linear elastic response. The same discussion also applies to the yield stress and hardening parameters of the FGC samples. It is noted that we determine the 'stress-strain' for FGC in order to compare the overall mechanical properties of FGC to those of the composites.

Table 4. Physical attributes of the FGC samples with layers of 0%, 5% and 10% Al_2O_3 volume content, used for compression testing at various testing temperatures

Test temp (^{0}C)	Sample	Mass (g)	Ht. (mm)	Dia (mm)	Porosity (%)
25	FGC-1	8.73	25.0	12.7	7.62
	FGC-2	8.19	24.2	12.7	4.87
200	FGC-3	8.22	24.5	12.7	4.85
400	FGC-4	8.33	24.9	12.7	5.55
	FGC-5	8.27	24.5	12.7	5.04

Table 5. Details obtained from the stress strain curves of the FGC samples tested at various temperatures

Test temp (^{0}C)	Sample	E (GPa)	σ_{yield} (MPa)	$\sigma_T = K\,\varepsilon_T^n$	
				K (MPa)	n
25	FGC-1	57.36	42	231.15	0.2867
	FGC-2	60.09	47	223.97	0.2648
200	FGC-3	57.64	34	200.07	0.2789
400	FGC-4	45.92	34	87.29	0.1560
	FGC-5	49.92	35	88.83	0.1557

From Table 5, the average modulus and yield stress for each FGC sample are calculated along with their standard deviation. Figure 7a-b shows the variation of the average elastic modulus and average yield stress with temperature for the FGC samples along with those of 0, 5 and 10 vol% composite samples. As expected, the elastic moduli and yield stresses of the FGC samples and the composite samples decreased significantly with increase in temperature. Further, the decrease in modulus with an increase in temperature was higher for the composite samples with uniform distributions of the constituents than that of the FGC samples. The FGC samples had higher modulus than the composite samples for all the volume fractions of the composite and for all the temperatures tested. This could be attributed to the fact that the FGC samples had slightly lower porosities than the composite samples. However, the trend is not that clear for the yield strength. FGC samples had higher yield strength than the composite samples, except at 200 ^{o}C.

To characterize the behavior in the strain-hardening region, it is necessary to determine the strain hardening coefficient (n) and strengthening coefficient (K) in the empirical model (Equation 1). Table 5 summarizes n and K values for all the FGC samples.

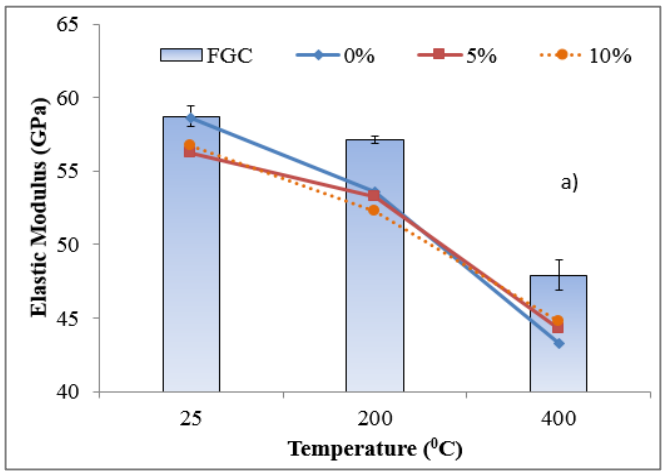

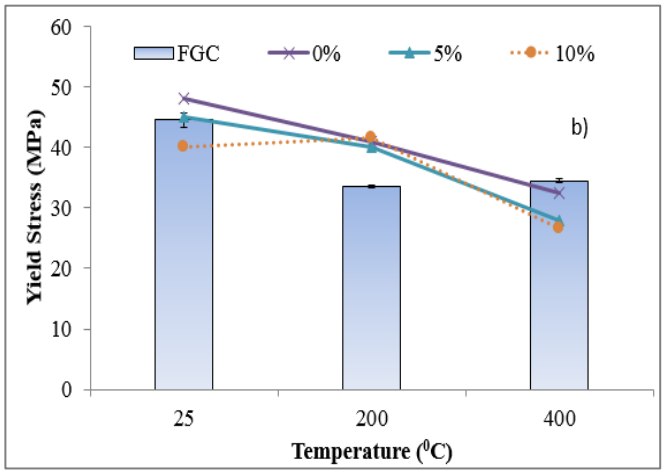

Figure 7. Effect of temperature on a) elastic modulus and b) yield stress of FGC and composite samples

Figure 8 shows the variation of strengthening coefficient (K) and strain hardening coefficient (n) with compression testing temperature for the FGC samples along with 0, 5 and 10 vol% composite samples. Both n and K decreased with increase in temperature, which is due to an increase in the dislocation mobility at higher temperatures making it easier for the materials to undergo plastic deformations, as it was previously discussed in the case of composite samples with homogeneous distribution of reinforcement phase. The FGC samples had n and K higher than the ones of the 0% samples, and further, with an increase in volume fraction, both n and K increased due to the hindrance provided by the alumina reinforcement for the dislocation motion.

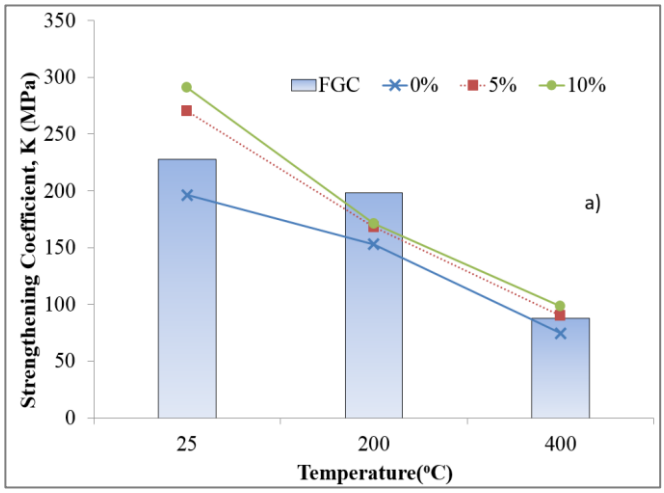

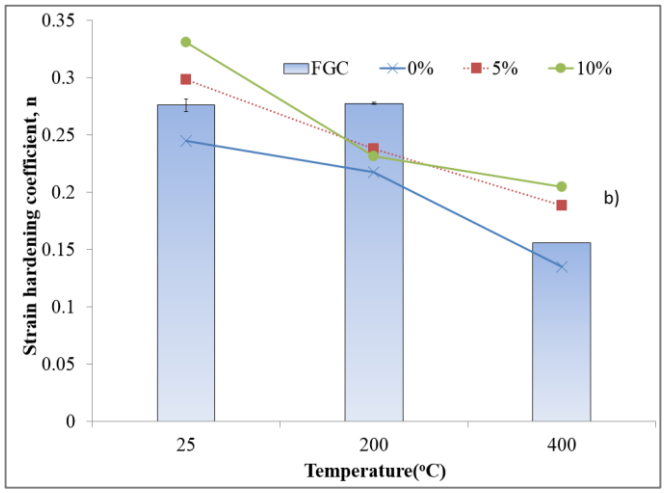

Figure 8. Effect of temperature on a) K and b) n of FGC and composite samples

5. Conclusion

We have studied the overall uniaxial mechanical response of Al-Al_2O_3 composite, with different alumina volume contents, and FGC samples at different isothermal temperatures (25, 200 and 400 °C) form their corresponding stress-strain curves. From the compression testing results, the effective moduli and yield stresses of the composites with uniform distributions of the Al and Al_2O_3 constituents were found to decrease with increase in temperature. However, with an increase in volume fraction of the alumina in the composite, the moduli and yield stresses were found to decrease because of an increase in the porosity of the samples with an increase in the alumina content. It is concluded that the overall mechanical response of the composites depends strongly on the temperature and porosity. Higher temperatures and increase in porosity reduce the elastic stiffness and load carrying capacity of the composites, as the composites become softer and easy to deform.

Functionally graded composite systems with alumina volume contents varying from 0 to 10% have been manufactured and tested for their compressive stress-strain responses. The FGC samples have almost identical response with those of 0% composite samples in the elastic region. However, the FGC samples showed slightly more strain hardening than the 0% samples, because of the hindrance to plastic deformation provided by the alumina reinforcement in the FGC samples. As expected, the moduli and yield strengths of the FGC samples and the composite samples decreased significantly with an increase in temperature because of increase in atomic vibrations and dislocation movement at higher temperatures. Further, the amount of reduction in the elastic moduli as temperature increases was

higher for the normal composite samples than that of the FGC samples.

To describe the inelastic behavior of the composites, we use an empirical model with the strain hardening coefficient (n) and strengthening coefficient (K). Higher values of n and K indicate higher rate at which the material strain hardens. The hardening parameters n and K decreased with increase in temperature for the FGC and composite samples. This is due to increase in the dislocation mobility at higher temperatures making it easier for the materials to undergo plastic deformations without much of strain hardening. The FGC samples had higher hardening parameters than the 0% samples, and further, with an increase in volume fraction, both hardening parameters increased due to the hindrance provided by the alumina reinforcement for the dislocation motion.

Acknowledgement

This research work was conducted with the support of US Air Force Office of Scientific Research (grant# FA 9550-10-1-0002) and National Science Foundation (grant# CMMI-1030836).

References

1. Saiz E, Tomsia AP and Suganuma K. Wetting and strength issues at Al/alpha-alumina interfaces. J Eur Ceram Soc. 2003; 23: 2787-96.
2. Nam TH. MMC Materialsearch. MMC-Assess. Vienna University of Technology, 2007, p. Assessment of Metal Matrix Composites for Innovations.
3. Surappa MK. Aluminium matrix composites: Challenges and opportunities. Sadhana-Acad P Eng S. 2003; 28: 319-34.
4. Kopeliovich D. Tribological properties of alumina reinforced composites. SubsTech, 2012.
5. Timsit RS, Waddington WG, Humphreys CJ and Hutchison JL. Structure of the Al/Al2O3 Interface. Appl Phys Lett. 1985; 46: 830-2.
6. Ali Hubi H, Newfal Z and Newal Muhammad D. Preparing and studying some mechanical properties of aluminum matrix composite materials reinforced by Al2O3 particles. Journal of Babylon University. 2012; 20: 30-8.
7. Kouzeli M and Dunand DC. Effect of temperature and strain rate on the compressive flow of aluminum composites containing submicron alumina particles. Metall Mater Trans A. 2004; 35A: 287-92.
8. Ganguly P. High temperature deformation and failure in aluminum-alumina particulate metal matrix composites. Department of Metals and Materials Engineering. The University of British Columbia, 1998.
9. Gudlur P, Boczek A, Radovic M and Muliana A. On Characterizing the Mechanical Properties of Aluminum-Alumina Composites. Materials Science and Engineering: A. 2013; 590: 352-9.
10. Yang Z, Zhang L, Shen Q and Gong D. Theoretical design of sedimentation applied to the fabrication of functionally graded materials. Metallurgical and Materials Transactions B. 2003; 34: 605-9.
11. Kieback B, Neubrand A and Riedel H. Processing techniques for functionally graded materials. Materials Science and Engineering: A. 2003; 362: 81-106.
12. Rajan T, Pillai R and Pai B. Characterization of centrifugal cast functionally graded aluminum-silicon carbide metal matrix composites. Materials Characterization. 2010; 61: 923-8.
13. Biesheuvel PM, Breedveld V, Higler AP and Verweij H. Graded membrane supports produced by centrifugal casting of a slightly polydisperse suspension. Chemical engineering science. 2001; 56: 3517-25.
14. Watanabe Y and Sato H. Review fabrication of functionally graded materials under a centrifugal force. Nagoya Institute of Technology, Japan. 2011.
15. Robson M, Blue C, Warrier S and Lin R. Sputter deposition of SiC coating on silicon wafers. Scripta metallurgica et materialia. 1992; 27: 565-70.
16. Fujii K, Imai H, Nomura S and Shindo M. Functionally gradient material of silicon carbide and carbon as advanced oxidation-resistant graphite. Journal of nuclear materials. 1992; 187: 204-8.
17. Shabana YM, Bruck HA, Pines ML and Kruft JG. Modeling the evolution of stress due to differential shrinkage in powder-processed functionally graded metal–ceramic composites during pressureless sintering. International Journal of Solids and Structures. 2006; 43: 7852-68.
18. Fukui Y, Takashima K and Ponton C. Measurement of Young's modulus and internal friction of an in situ Al-Al3Ni functionally gradient material. Journal of materials science. 1994; 29: 2281-8.
19. Ben-Oumrane S, Abedlouahed T, Ismail M, Mohamed BB, Mustapha M and El Abbas AB. A theoretical analysis of flexional bending of Al/Al2O3 S-FGM thick

beams. Computational Materials Science. 2009; 44: 1344-50.

20. Gudlur P, Forness A, Lentz J, Radovic M and Muliana A. Thermal and mechanical properties of Al/Al203 composites at elevated temperatures. Materials Science and Engineering A. 2011.
21. Callister WD and Rethwisch DG. Fundamentals of materials science and engineering: an integrated approach. John Wiley & Sons, 2012.
22. Groover MP. Fundamentals of modern manufacturing: materials processes, and systems. John Wiley & Sons, 2007.
23. Askeland DR, Fulay PP and Wright WJ. The science and engineering of materials. Thomson Engineering, 2011.
24. Totten GE and Mackenzie DS. Handbook of aluminum: vol. 1: physical metallurgy and processes. CRC, 2003.
25. Radovic M, Lara-Curzio E and Riester L. Comparison of different experimental techniques for determination of elastic properties of solids. Materials Science and Engineering A. 2004; 368: 56-70.